LONGSHORE SEDIMENT FLUX IN WATER COLUMN AND ACROSS SURF ZONE

By Ping Wang[1]

ABSTRACT: Streamer sediment traps were used to measure the distribution of longshore sediment flux in the surf zone at 29 locations along the southeast coast of the United States and the Gulf coast of Florida. Measurements were conducted on both barred and nonbarred coasts under low-wave energy conditions. Results indicate that longshore sediment flux decreases logarithmically upward in the water column throughout the surf zone, and the rate of upward decrease is largest in the trough and smallest in the swash due to stronger mixing energy in the swash. Six types of cross-shore distribution patterns of longshore sediment transport (LST) were found. These six distribution patterns are controlled by nearshore morphology, breaker type, and energy dissipation pattern. For low-wave energy coasts, the swash (nonbarred coast) and inner surf (barred coast) zones contain significant contributions to the longshore sediment transport rate. The cross-shore distribution pattern of the longshore sediment transport rate along nonbarred coasts was well reproduced using energy-dissipation and shear-stress approaches developed mainly from laboratory studies.

INTRODUCTION

Longshore sediment transport (LST) and its distribution in the water column and across the surf zone are central to effective design of beach nourishment, groins, jetties, and many other coastal structures. Field data are essential for testing and improving models of three-dimensional sediment transport to increase our ability to predict anthropogenic impacts on natural variability in the coastal zone. Insight into the distribution of LST is also helpful to further our understanding of spit development and the migration of natural or artificially placed shoreline features.

Suspended sediment concentration under breaking and nonbreaking waves has been the subject of numerous studies (Kana 1979; Nielsen 1984a,b, 1986; Bosman et al. 1987; Sternberg et al. 1989; Zampol and Inman 1989; Barkaszi and Dally 1993). One of the main purposes of suspended-sediment measurement is for the calculation of the sediment flux

$$F(x) = \frac{1}{T}\int_0^T \int_0^h U(z, t)C(z, t)\, dz\, dt \qquad (1)$$

where $F(x)$ = sediment flux throughout the water column at location x, averaged over a time interval of T (e.g., one wave period); U = particle velocity (alongshore, in this case) as a function of depth z and time t; and C = suspended sediment concentration. Within the surf zone, it is difficult to measure U and C simultaneously at the same location, and it is even more difficult to measure them instantaneously with respect to depth.

Existing field data on longshore sediment flux and its distribution in the water column and across the surf zone are scarce. Most of the existing sediment tracer measurements (Komar and Inman 1970; Duane and James 1980) concentrated on the total rate of LST. Unless multicolor tracers are used (Kraus et al. 1983), the cross-shore distribution of LST cannot be reliably measured. Impoundment at coastal structures has been used to evaluate LST relationships developed mainly from sediment tracer studies (Dean 1989). Except for a few well-controlled short-term impoundment studies (Bodge 1986; Bodge and Dean 1987), this technique is generally not capable of providing transport distribution information.

In the present study, streamer sediment traps (Kraus 1987) were used to measure longshore sediment flux and its distribution in the surf zone. Field measurements were conducted at 29 sites along the southeast coast of the United States and the Gulf coast of Florida. The measurements were conducted on both barred and nonbarred coasts under low wave-energy conditions. The longshore sediment flux was measured throughout the water column in different locations in each surf zone (Fig. 1). The objective of this study is to characterize the various distribution patterns of longshore sediment flux in the water column and across the surf zone. Empirical modeling of the vertical and horizontal distribution patterns is also discussed.

STUDY AREAS AND METHODOLOGY

Field experiments were conducted from September 1993 to May 1995 (Fig. 1). Seven of the 29 measurements were located on barred coasts with waves breaking on the bar. Eighteen were on coasts with negligible offshore bar influence on wave breaking. Four measurements were conducted in the inner surf zone (Table 1) on barred coasts due to operational difficulties caused by high-wave energy and a deep trough. Twelve field sites had a plunge step at the breaker line or secondary breaker line for the barred coasts. Sediment grain-size varied from beach to beach as well as from one part of a beach to another (Wang 1995). The mean grain-size variation

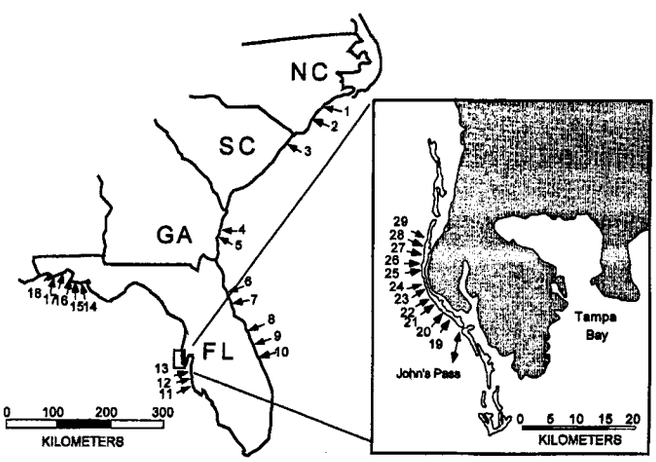

FIG. 1. Study Areas along Southeast Atlantic and Northeast Gulf of Mexico

[1]Asst. Prof. of Res., Coast. Studies Inst., Louisiana State Univ., 331 Howe/Russell Geoscience Complex, Baton Rouge, LA 70803.

Note. Discussion open until November 1, 1998. To extend the closing date one month, a written request must be filed with the ASCE Manager of Journals. The manuscript for this paper was submitted for review and possible publication on March 21, 1997. This paper is part of the ***Journal of Waterway, Port, Coastal, and Ocean Engineering***, Vol. 124, No. 3, May/June, 1998. ©ASCE, ISSN 0733-950X/98/0003-0108–0117/$8.00 + $.50 per page. Paper No. 15397.

TABLE 1. Summary of Hydrodynamic and Morphodynamic Conditions at Field Sites

Location and site identification (1)	Number of trap arrays (2)	Surf zone width (m) (3)	Beach slope[b] (4)	Average grain size[d] (mm) (5)	H_{rms} (m) (6)	Incident wave angle (deg) (7)	Wave period (s) (8)
1. Emerald Isle, N.C.	4	35	0.028	0.35	0.79	13.5	7.5
2. Onslow Beach, N.C.	3	7[c]	0.094	2.25	0.61	12.0	6.0
3. Myrtle Beach, S.C.	5	24	0.030	0.26	0.51	4.0	8.5
4. Jekyll Island, Ga.	2	9	0.044	0.17	0.20	3.0	3.5
5. Jekyll Island, Ga.	3	14	0.033	0.26	0.35	10.0	3.3
6. Anastasia Beach, Fla.	6	36	0.013	0.19	0.49	5.5	10.5
7. N. Mantazas Beach, Fla.	3	14	0.031	0.28	0.44	7.2	7.2
8. Canaveral Seashore, Fla.	3	6[c]	0.115	0.90	0.46	9.0	3.5
9. Melbourne Beach, Fla.	2	4[c]	0.158	1.50	0.50	2.5	3.5
10. Beverly Beach, Fla.	2	3[c]	0.161	0.41	0.36	11.5	3.5
11. Lido Key Beach, Fla.	4	38	0.105	0.68	0.38	14.0	3.7
12. Lido Key Beach, Fla.	5	35	0.101	0.54	0.34	19.0	3.4
13. Lido Key Beach, Fla.	4	21	0.101	0.37	0.21	2.6	3.0
14. St. George Island, Fla.	3	3	0.123	0.29	0.29	35.3	3.0
15. St. George Island, Fla.	4	4	0.214	0.41	0.22	31.5	2.9
16. St. George Island, Fla.	3	2	0.129	0.43	0.28	23.0	3.0
17. St. Joseph Island, Fla.	4	10	0.062	0.24	0.53	9.3	4.2
18. Grayton Beach, Fla.	4	29	0.042	0.28	0.56	8.5	4.5
19. Redington Beach, Fla.	3	4	0.125	0.85	0.36	8.4	4.5
20. Redington Beach, Fla.	3	11	0.035	0.20	0.28	10.7	3.9
21. Redington Beach, Fla.	4	19	0.026	0.90	0.32	19.2	4.5
22. Redington Beach, Fla.	4	17	0.016	0.43	0.24	15.8	4.9
23. Redington Beach, Fla.	4	54	0.014	0.37	0.69	13.1	7.3
24. Indian Shores, Fla.	3	12	0.039	0.32	0.36	20.0	4.5
25. Indian Shores, Fla.	1	4	0.082	0.40	0.31	1.8	3.3
26. Indian Rocks Beach, Fla.	2	4	0.072	0.28	0.36	7.7	2.9
27. Indian Rocks Beach, Fla.	3	7	0.066	0.42	0.34	7.5	4.2
28. Indian Rocks Beach, Fla.[a]	2	2	0.141	1.38	0.19	10.0	2.8
29. Indian Rocks Beach, Fla.[a]	2	2	0.152	1.29	0.14	8.2	3.8

Note: See Fig. 1 for study areas along southeast Atlantic and northeast Gulf of Mexico.
[a]Simultaneous impoundment and sediment trapping.
[b]Determined from breaker line to shoreline.
[c]Number indicates width of inner surf zone, unable to perform trapping in trough or on bar due to rough conditions.
[d]Average of surface samples collected at each trap location.

on one of the beaches were as large as 3.71 mm, 4.06 mm at the breaker line and 0.35 mm in the trough.

The streamer sediment traps (Kraus 1987; Rosati and Kraus 1988, 1989) used to measure the longshore sediment flux and its distribution across the surf zone had openings of 15 × 9 cm (Fig. 2), and the distance between two adjacent streamer bags was 6 cm. The mesh size of the sieve cloth from which the streamers were made was 63 μm. An array of streamer traps was mounted on a rack constructed of polyvinyl chloride (PVC) pipes. Traps of different lengths were used at different water levels. Longer traps (~120 cm) were used at the bottom three levels and shorter traps (~70 cm) were used at higher levels. This design allowed good coverage throughout the water column, easy assembly, and efficient sediment sampling and retrieval (Wang and Davis 1994; Wang 1995).

Four to eight streamer bags were mounted on each rack as determined by the water depth and breaker height. This assemblage is called one trap array in the following discussion. Each field experiment was composed of three to six streamer-trap arrays across the surf zone. The placement of streamer-trap arrays in the surf zone was based on morphologic and hydrodynamic conditions. The general placement for a barred coast was one trap array on top of the bar, one in the trough, one at the secondary breaker line, and one in the swash. On a nonbarred coast, the commonly used streamer-array arrangement was one at the breaker line, at least one in the surf bore area and one in the swash.

Beach profiles and locations of trap arrays were surveyed using standard level and transit procedures with an electronic total station. Still water level was estimated at the time of the survey. Breaker height and wave period were measured using

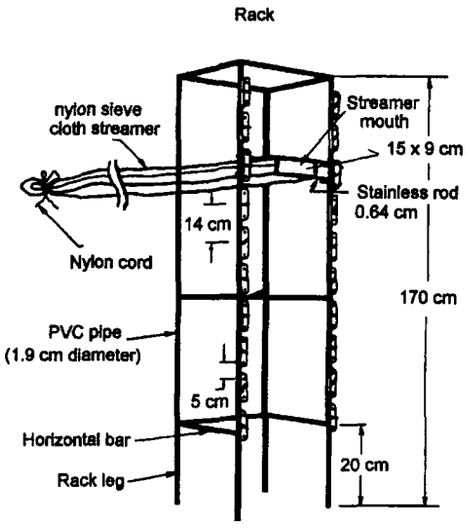

FIG. 2. Design of Streamer Traps and Supporting Rack [Modified from Kraus (1987)]

an array of scaled photopoles (Ebersole and Hughes 1987) placed at the same locations as the trap arrays. Incident breaking wave angle was estimated using a hand-held compass. A bottom sediment sample was collected at each trap-array location. The trapping duration was determined based on the magnitude of the LST rate and the trapping conditions. The duration was typically 5 min. Under high-wave energy and/or high-transport conditions, the duration was shortened to 3 min.

Sediment flux between two adjacent streamer bags was obtained through linear integration

$$\Delta F_i = \frac{\left[\left(\frac{F_{i+1}}{b_{i+1}}\right) + \left(\frac{F_{i-1}}{b_{i-1}}\right)\right] \Delta b_i}{2} \quad (2)$$

where ΔF = sediment flux between two adjacent streamers; F_{i+1} and F_{i-1} = flux through the upper and lower streamers, respectively; b_{i+1} and b_{i-1} = streamer opening heights of the upper and lower streamer mouths, respectively. They are both 9 cm for the traps used in this study (Fig. 2); and Δb = distance between the two adjacent streamers, which equals 6 cm for the racks used in this study. A similar algorithm was used by Kraus et al. (1989b) and Rosati et al. (1990, 1991). The bottom of the lowest streamer trap was placed on the seabed at the beginning of the trapping procedure. A scour hole 1–3 cm deep was sometimes observed toward the end of the experiment. The total sediment flux throughout the water column at a certain trap-array location was obtained by summing the flux through each streamer and that in between the streamers.

RESULTS AND DISCUSSION

One hundred and six longshore sediment flux profiles were measured at the 29 field sites. Each flux profile, typically representing an average of 5 min was composed of 3–8 measurements throughout the water column. The distribution of LST rate across the surf zone was measured by 2–6 streamer-trap arrays (Table 1).

Sediment-Flux Profiles in Water Column

The longshore sediment flux decreased upward in the water column (Fig. 3). The upward decreasing trend was approximately logarithmic throughout the surf zone: in the swash, at the breaker line, in the trough, and on the breaker-point bar. The logarithmic decrease of the sediment flux can be explained by the existing understanding of profiles of sediment concentration and longshore-current velocity. Many studies have shown that sediment concentration decreases logarithmically upward (Bosman 1987; Nielsen 1984b, 1986). The velocity profile has been found to be fairly constant throughout the water column except in the thin bottom-boundary layer (Deigaard et al. 1986). The product of a logarithmic concentration profile and a uniform velocity profile results in the logarithmic flux profile. Similar logarithmic sediment-flux profiles were also measured by other streamer trap studies (Kraus et al. 1989a; Rosati and Kraus 1989; Rosati et al. 1990).

Calculating Longshore Sediment Flux in Water Column

Kraus and Dean (1987) and Kraus et al. (1989a) proposed a formulation to describe the sediment-flux profile in the water column

$$F(x, z) = F_0(x)P(x, z) \quad (3)$$

where $F_0(x)$ = magnitude function, assumed to depend on local wave, current, water depth, and beach conditions (Kraus et al. 1989a); z = elevation above bed; and $P(x, z)$ = dimensionless shape function. Kraus and Dean (1987) found that $P(x, z)$ can be described as

$$P(x, z) = \exp\left(-\alpha\left(\frac{z_{ci}}{h(x)}\right)\right) \quad (4)$$

where α = dimensionless empirical coefficient; z_{ci} = height of the trap center above the bottom; and $h(x)$ = water depth at the trap-array location.

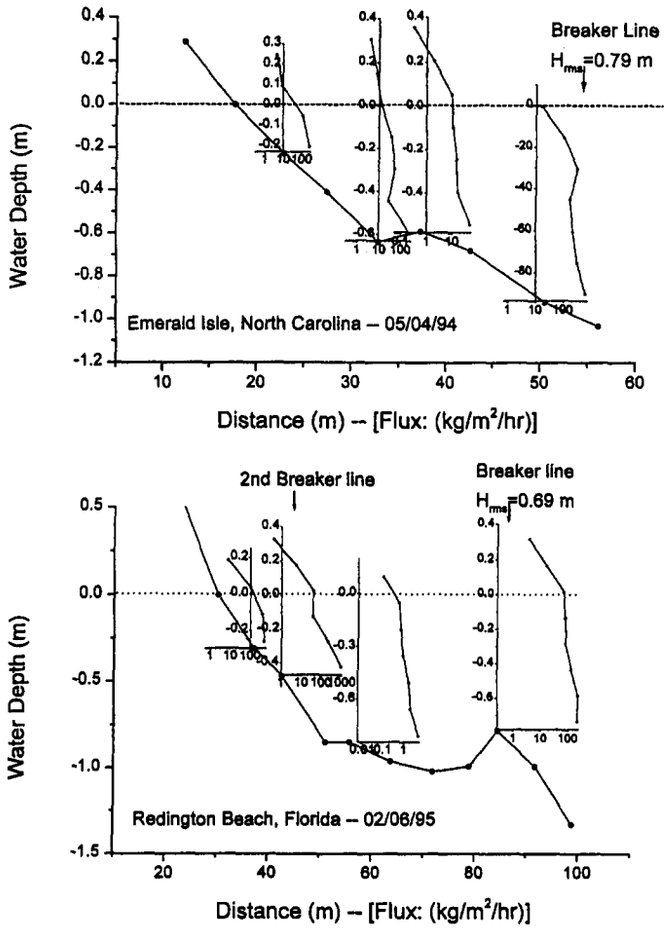

FIG. 3. Examples of Field Measurement. Zero Water Level Was Estimated at Time of Experiment

TABLE 2. Shapes of Longshore Sediment Flux Profiles in Water Column

Morphological feature (1)	Number of profiles (2)	Average α (3)	Standard deviation, α (4)	Average correlation, R (5)
Swash	25	2.0	0.6	0.94
Breaker line	41	2.9	0.9	0.94
Trough	10	3.2	1.1	0.86
Bar	14	2.9	0.5	0.93
Bore (nonbar)	9	3.1	0.6	0.95
Outside surf	7	2.7	1.7	0.85
Average [Total]	[106]	2.7	0.9	0.93

Note: Individual α values were found through regression analysis to each measured sediment flux profile.

The shape of the profile [(4)], that describes how rapid the longshore sediment flux decreases upward, is determined largely by the value of the coefficient α. A larger α value corresponds to a greater rate of upward decrease, and a smaller α value leads to a smaller rate of upward decrease, given the same dimensionless depth (z_{ci}/h). Eq. (4) was best-fit to each of the measured vertical flux profiles. It was found that the α values were different in different parts of the surf zone (Table 2). The rate of sediment-flux decrease was generally smaller in the swash zone than in other parts of the same surf zone. This is explained by the shallower water and stronger mixing in the swash. The rate of upward decrease was greatest in the trough, caused by the least mixing energy. The average α value of about 2.7, found for the entire surf zone in the present study, was also obtained in studies conducted by Kraus et al. (1989a) and Rosati et al. (1991).

Significant amounts of sediment were transported above the mean zero water level at the time of the experiment (Fig. 3). This is because the streamer bags located above the zero water level were temporarily submerged when the wave crests passed the trap array. Sediments were thus trapped in the streamers above the zero water level. Similar observations were made by Kraus et al. (1989a) and Kraus and Dean (1987). As expected, sediment transport above the zero water level was more significant in the swash zone than in the other parts of the surf zone.

The magnitude of sediment flux in the water column is controlled by the magnitude function $F_0(x)$ in (3). Theoretically, $F_0(x)$ is determined by the mechanics of sediment suspension and longshore transport. Factors may include bottom shear stress, turbulence length and intensity, sediment diffusivity, sediment fall velocity, and longshore current velocity. The present understanding of the preceding factors and their interactions in the surf zone is insufficient to develop a general model. In the following sections, three candidate approaches are examined to empirically determine the magnitude function based on the field data: (1) longshore energy flux, (2) energy dissipation, and (3) bottom shear stress.

Uniform Longshore Energy Flux

It has been found that the total rate of LST in the surf zone is proportional to the longshore energy flux factor at the breaker line (*Shore* 1984; Komar 1990; Bodge and Kraus 1991; Wang et al. 1998). The magnitude function, $F_0(x)$, is assumed to be proportional to the longshore energy flux per unit surf-zone area

$$F_0(x) = K_\phi \left(\frac{P_l}{gA_{sf}}\right) \tag{5}$$

where K_ϕ = dimensionless proportionality constant; A_{sf} = cross-sectional area of the surf zone; g = gravitational acceleration; and P_l = longshore energy flux factor expressed as

$$P_l = \frac{1}{16}\rho g H_b^2 \sqrt{g h_b}\,\sin(2\theta_b) \tag{6}$$

where ρ = fluid density; H_b = breaker height; h_b = breaking water depth; and θ_b = breaking wave angle. Realizing that the magnitude of energy flux varies across a surf zone, the calculation of the magnitude function, $F_0(x)$, was adjusted by assigning different K_ϕ values to different portions of the same surf zone. It is further assumed that the longshore energy flux per unit area is uniform in specific parts of a surf zone, such as the swash zone, breaker line, trough, and bar crest. Average K_ϕ values obtained for the swash zone, breaker line, trough, and bar crest are used to calculate $F_0(x)$.

The $F_0(x)$ value for the measured flux profile is obtained through regression analysis. The calculated [(5)] and measured $F_0(x)$ values are compared in Table 3. Examples of best fit, worst underprediction, and worst overprediction are shown in Fig. 4. The rather large variations of $F_0(x)_{predicted}/F_0(x)_{measured}$ indicate that the predictions are fairly poor. Larger K_ϕ values were found in the swash and at the breaker line, where more sediment is transported, than in the surf bore area and trough.

TABLE 3. Comparison between Measured and Predicted $F_0(x)$ Values from Energy Flux and Energy Dissipation

Morphological features (1)	Best-fit (2)	Number of profiles (3)	$F_0(x)_{predicted}/F_0(x)_{measured}$ Highest (4)	Lowest (5)	Standard deviation (%) (6)
(*a*) Energy flux approach					
Breaker line[a]	95, K_ϕ	25	3.32	0.07	83
Swash[b]	127, K_ϕ	23	4.28	0.10	109
Bore area[c]	45, K_ϕ	8	4.50	0.04	144
(*b*) Energy dissipation approach					
Breaker line[a]	7.7, K_2	25	5.24	0.07	126
Swash[b]	11.9, K_2	21	8.44	0.04	166

Note: Proportional constants K_ϕ [(5)] and K_2 [(10)] were adjusted for different parts of the surf zone.
[a]Including the second breaker for barred beach.
[b]Including both barred and nonbarred beach.
[c]Midsurf area for nonbarred beach.

TABLE 4. Comparison between Measured and Predicted $F_0(x)$ Values from Bed-Shear-Stress Approach

Prediction (1)	Constant K_4 (2)	Constant K_2 (3)	Standard deviation[a] (4)
Eq. (14)	0.014	0	73
Eq. (16)	K_6, k_3 0.014, 1.02	k_4 0	73

Note: Proportional constants K_ϕ [(5)] and K_2 [(10)] were adjusted for different parts of surf zone.
[a]Percent of mean $F_0(x)_{predicted}/F_0(x)_{measured}$ that was adjusted to 100%.

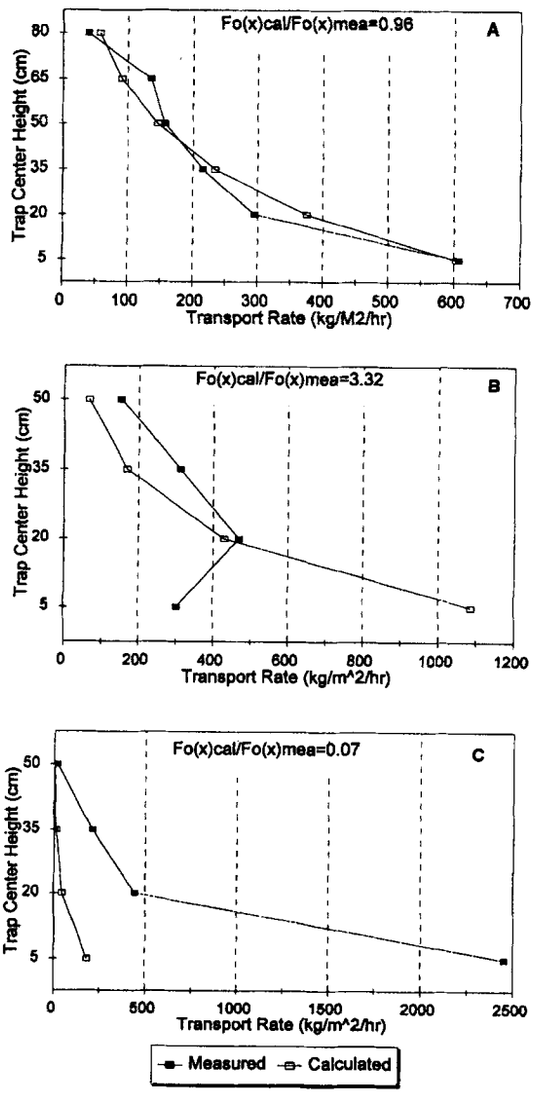

FIG. 4. Measured and Predicted Flux Profiles from Energy-Flux Approach at Breaker Line: (a) Best Fit, Emerald Isle, N.C.; (b) Worst Overprediction, Lido Key, Fla.; (c) Worst Underprediction, Beverly Beach, Fla.

Energy Dissipation

This approach assumes that the magnitude function $F_0(x)$ can be determined by the product of longshore current velocity (V) and the rate of energy dissipation expressed in the term of wave decay (dH_b/dx)

$$F_0(x) = K_1 \rho V \frac{dH_b}{dx} \tag{7}$$

where K_1 = dimensionless proportional constant. The empirical formula developed by Komar and Inman (1970) was used to estimate the longshore current velocity

$$V_{ms} = 1.17\sqrt{gh_b} \sin \theta_b \cos \theta_b \tag{8}$$

where V_{ms} = longshore current velocity at midsurf position. Assuming a constant ratio of breaker height and water depth, the wave decay term can be simplified as

$$\frac{dH_b}{dx} = \frac{d(\gamma h)}{dx} = \gamma \frac{dh}{dx} \tag{9}$$

The magnitude function, $F_0(x)$, can then be calculated as

$$F_0(x) = K_2 \gamma \rho \sqrt{gh_b} \sin \theta_b \cos \theta_b \frac{dh}{dx} \tag{10}$$

where K_2 = dimensionless empirical constant; γ = ratio of breaker height versus breaking water depth; and dh/dx = local bed slope.

Eq. (10) was used to calculate $F_0(x)$ in the swash zone and at the breaker line. The predicted and measured results are compared in Table 3. The large variations of $F_0(x)_{predicted}/F_0(x)_{measured}$ indicate an overall poor prediction by this approach. The poor match with the field data might be caused by the longshore current velocity prediction. Eq. (8) (Komar and Inman 1970) is believed to provide a reasonable estimate of the longshore-current velocity at the midsurf location; however, the cross-shore distribution of the longshore current is not included. Part of the inconsistency could also be caused by the assumption of a constant ratio of breaker height and water depth, which simplified the energy dissipation to be represented by local bed slope.

Bottom Shear Stress

It has been demonstrated that bed-load transport and suspension of sediment are proportional to the excess bed-shear stress or a power function of the shear stress (Van Rijn 1984). It is assumed that the magnitude of the sediment flux can be determined by the product of excess shear stress and longshore current velocity

$$F_0(x) = K_3(\Psi - \Psi_c)V \left(1 + \frac{dH_b}{dx}\right)^{k_1} \tag{11}$$

where Ψ and Ψ_c = actual and critical shear stress, respectively, expressed in the form of the Shields parameter; and K_3 and k_1 = dimensionless empirical constants.

The shear-stress approach was applied to calculate the 23 sediment-flux profiles measured at the breaker line. The reason that the breaker-line profiles were selected was that the variables in (11) could be determined with more confidence at the breaker line than in other areas in the surf zone. The wave Shields parameter Ψ was determined as

$$\Psi = \frac{C_f H_b^2}{8h_b(s - 1)d} \tag{12}$$

where C_f = wave friction coefficient; s = ratio of sediment density to water density; and d = sediment grain size. For typical beach sand, the critical Shields parameter Ψ_c was found to be about 0.05 (Madsen and Grant 1976). The longshore-current velocity at the breaker line was determined based on Longuet-Higgins' (1970) analysis assuming no lateral mixing

$$V_0 = \frac{5\pi}{16} \gamma \zeta \frac{m}{C_f} (gh_b)^{1/2} \sin(2\theta) \tag{13}$$

where V_0 = longshore current velocity; m = beach slope in the surf zone; and $\zeta = 1/(1 + 3\gamma^2/8)$. The rate of wave-energy dissipation was determined through local beach slope by assuming a constant breaker index, γ.

The actual Ψ was much larger than the critical Ψ_c under breaking-wave conditions. Ψ_c was therefore neglected and eliminated from (11). Substituting Ψ [(12)] and V_0 [(13)] into (11), and multiplying sediment density ρ_s to achieve consistent dimension, gives

$$F_0(x) = K_4 \frac{\sqrt{g}H_b^2 m \sin(2\theta_b)}{\sqrt{h_b}(s - 1)d} \left(1 + \gamma \frac{dh}{dx}\right)^{k_2} \rho_s \tag{14}$$

where K_4 and k_2 = dimensionless constants. The wave friction coefficient, C_f, was canceled during the calculation of shear stress [(12)] and longshore current velocity [(13)].

It has been demonstrated that the suspension of sediment is proportional to a power function of excess bed-shear stress (Van Rijn 1984). Eq. (11) was modified to examine the relationship between the power function and the longshore-sediment flux

$$F_0(x) = K_5 \rho_s (\Psi - \Psi_c)^{k_3} V \left(1 + \frac{dH}{dx}\right)^{k_4} \tag{15}$$

Substituting Ψ [(12)] and V_0 [(13)] into (15) and neglecting the critical shear stress, (15) becomes

$$F_0(x) = K_6 \rho_s \left(\frac{C_f H^2}{h_b(s - 1)d}\right)^{k_3} \frac{m}{C_f} \sqrt{gh_b} \sin(2\theta_b) \left(1 + \frac{dh}{dx}\right)^{k_4} \tag{16}$$

where K_6, k_3, and k_4 = dimensionless empirical coefficients. The wave friction coefficient, C_f, was determined based on the analysis of Jonsson (1966) and Sunamura and Kraus (1985).

Eqs. (14) and (16) were applied to calculate the $F_0(x)$ at the breaker line. The calculated and measured $F_0(x)$ values are summarized in Table 4. The more complicated (16) failed to provide more accurate prediction than the simpler (14). The advantage of using (14) is that the calculation of the poorly understood wave friction factor is avoided.

In summary, although the field data were reproduced the best by the shear-stress approach among the previous three analyses, the overall prediction was still not satisfactory. A wave-by-wave description instead of time-averaged values, as well as a realistic description of turbulence intensity (e.g., breaker type) and sediment-water interactions, is likely necessary for the sediment-flux modeling.

Distribution of Longshore Sediment-Transport Rate across Surf Zone

The measured cross-shore distribution of the LST rate is not uniform. Several transport patterns have been found by previous field and laboratory studies (Kraus et al. 1989a; Bodge 1986; Kamphuis 1991b). Among influential factors, the longshore-current distribution, water depth, bed slope, energy-dissipation rate, and sediment grain size are believed to be significant.

Only three of the 27 multitrap measurements showed a fairly uniform transport-rate distribution. The majority of the measured distributions had an obvious transport peak. For the convenience of discussion, the transport peak is arbitrarily defined here as the rate that is at least two times greater than

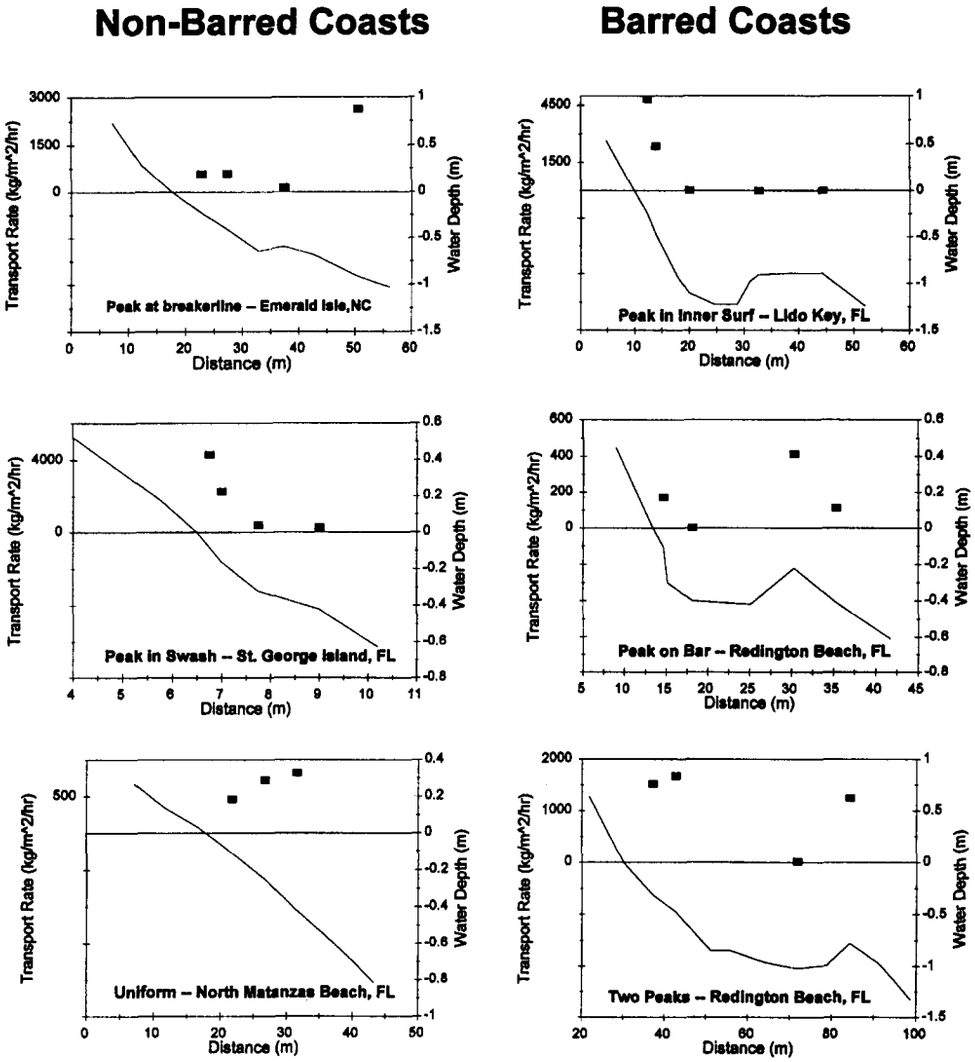

FIG. 5. Cross-Shore Distribution Patterns of Longshore Sediment Transport

rates measured by adjacent trap arrays. Various cross-shore distribution patterns were measured (Fig. 5).

The field data indicate that swash (nonbarred coast) and inner surf (barred coast) zones are important controlling areas for the LST along the low wave-energy coasts (Table 5). The significance of swash contributions to total LST rate has been emphasized in several previous studies, including both field (Kraus et al. 1983; Bodge 1986; Bodge and Dean 1987; Kraus and Dean 1987) and laboratory experiments (Bodge 1986; Kamphuis 1991b).

The uniform distribution of the LST was measured on three nonbarred beaches, each with a relatively narrow surf zone and uniform beach slope. Uniform energy dissipation was observed in the field. Breaker type was between plunging and spilling.

For nonbarred coasts, the pattern with a peak in the swash (Fig. 5; Table 5) was typically found in the narrow surf zone with collapsing breakers. The surf-bore area was usually narrow or nonexistent, a significant amount of wave energy was dissipated in the swash immediately after the waves broke. Waves were usually chaotic without a distinct breaker line. Bodge (1986) also found from laboratory impoundment experiments that under collapsing breakers, a significant amount of sediment was transported in the swash zone.

The pattern with a peak at the breaker line was usually found in wide surf zones with plunging breakers. A significant amount of energy was dissipated at the breaker line. The energy was further dissipated in the wide surf-bore area such that most of the energy had already been dissipated by the time the breaking waves reached the swash zone. The pattern with a peak at the breaker line was also found in some of the narrow surf zones with plunging breakers. This peak was prob-

TABLE 5. Cross-Shore Distribution of Longshore Transport Rate in Surf Zone, Described in Terms of Morphological Features

Description (1)	Number of field sites (27 measurements) (%) (2)
Uniformly distributed	3 (11)
Beach without bar	
Peak in swash	8 (30)
Peak at breaker line[a]	5 (19)
Beach with bars	
Peak on the bar	1 (4)
Peak in inner surf[b]	8 (30)
Peaks on bar and in inner surf	2 (7)

[a]Peak is actually a short distance landward of breaker line.
[b]Four peaks were estimated from field observation during measurement, trappings were not able to perform on the bar due to rough conditions and deep water.

ably caused by the fact that most of the waves were breaking at almost exactly the same location, forming a distinctive breaker line. Morphologically, these beaches all had a steep plunge step.

Most barred coasts had transport peaks in the inner surf zone. This was partly an artifact of the low wave-energy conditions encountered in this study. Most of the measurements on barred coasts were conducted under normal weather, and only some of the larger waves broke on the bar. These were mostly of the spilling type, and suspended sediment concentration in the water column was low. This was confirmed by the wave ripples that were observed on top of the bars, indicating lower flow regime at the bottom boundary layer as compared to the upper-regime plane bed in the inner surf zone (Clifton 1976). The small waves and reformed waves from the bar breakers broke in the inner surf zone as secondary breakers resulting in significant sediment transport. The one case when a transport peak was measured on the bar crest was during a spring low tide when the water depth on top of the bar was extremely low, resulting in dissipation of most wave energy on top of the bar. The secondary breakers carried a limited amount of energy, and were not capable of transporting a significant amount of sediment. This indicates that tidal level may have a significant influence on the cross-shore distribution of LST.

The one case with two transport peaks was measured during a storm with chaotic wave conditions. Significant wave breaking took place both on top of the bar and in the inner surf zone resulting in large amounts of sediment transport in both locations.

Cross-Shore Distribution of Longshore Transport and Sediment Size

The cross-shore distribution of sediment grain-size may contain considerable information on transport processes. Grain sizes have significant influence on bottom shear stress and, hence, the initiation of sediment movement. Sediment fall velocity is one of the factors that controls the suspended sediment transport. On the other hand, it is the transport processes, i.e., waves and currents, that sort and redistribute the sediment across the surf zone.

The peak of LST usually occurred in the place where the coarsest sediment was found [Fig 6(a)]. An important point, however, is that grain-size distribution across the surf zone is also controlled by the character of the available sediment. For beaches with uniform sediment grain size, little information on transport distribution can be inferred from the sediment grain size [Fig. 6(b)].

The correspondence of the transport peak and the coarsest sediment size can be explained by the intensity of sediment transport processes; higher energy is capable of transporting coarser and more sediment. On the other hand, fine sediment cannot be deposited above a certain energy level, leaving only coarser sediment on the bottom. Finer sediments are ultimately deposited at points of lesser turbulence (Bascom 1951), e.g., in the trough of a bar. The cross-shore movement of breaking waves has significant influence on the grain-size distribution, it is this motion that initiates the sediment movement for LST.

Distribution of Longshore Sediment Transport and Local Bed Slope

Local bed slope has significant influence on the rate of wave-energy dissipation (Dally et al. 1985). Wave energy and its dissipation rate also influence the local bed slope. Bascom (1951) found that beaches that were protected, e.g., with an offshore bar, were steeper for any given sand size than exposed beaches, i.e., facing the open ocean.

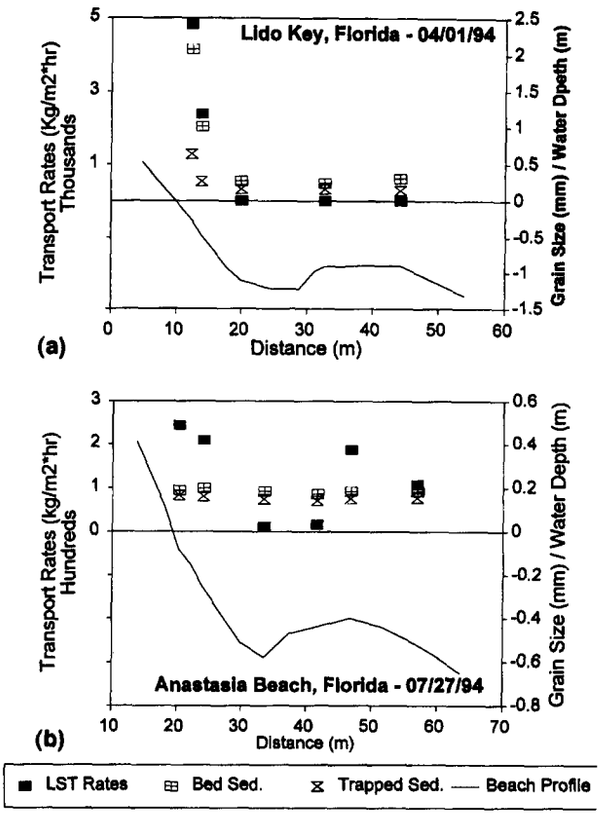

FIG. 6. Distributions of LST Rates and Grain Sizes of Bottom and Trapped Sediments: (a) Higher LST Rate Corresponds to Coarser Sediment, Lido Key, Fla.; (b) Relationship Is Not Distinctive due to Uniform Sediment, Anastasia Beach, Fla.

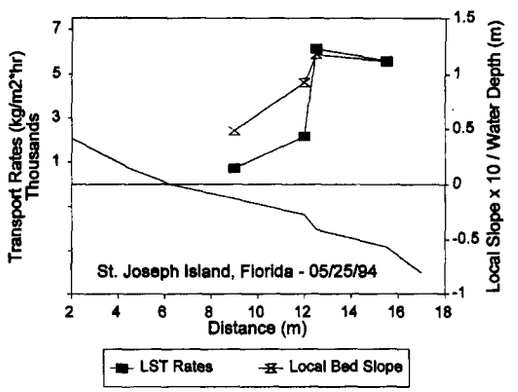

FIG. 7. Relationship between LST Rate and Local Bed Slope, Higher LST Rates Correspond to Steeper Bed Slope, St. Joseph Island, Fla.

The field data presented here imply that a higher LST rate is usually related to a steeper slope (Fig. 7), which results in a greater rate of energy dissipation (Dally et al. (1985) and, thus, a larger rate of sediment transport. Bodge (1986) also found a correlation between local seabed slope and LST. Valuable information on the cross-shore distribution pattern of LST can be inferred from the local bed slopes that are easier to measure than the transport rate. It is worth mentioning, however, that both LST and local bed slope can be affected by other factors, such as grain-size and breaker type (Wang and Davis, in press, 1998).

Calculating Cross-Shore Distribution Pattern of Longshore Sediment Transport

Compared to the numerous models used to predict the total rate of LST (Komar and Inman 1970; Bailard 1981; Kamphuis

et al. 1986; Kamphuis 1991a; Bodge and Kraus 1991; Wang et al., 1998), models incorporating cross-shore distribution of LST (Thornton 1973; Bodge 1986, 1989; Watanabe 1993) are scarce and poorly verified due to the lack of data, particularly field data. Most existing models assume a plane beach. Two of the distribution models, the Bodge (1986) model using an energy-dissipation approach and the Watanabe (1993) model using a shear-stress approach, are examined using the present field data. Six of the 29 field sites are close to the plane beach assumption and examined.

Simplified Bodge (1986) Model—Energy Dissipation

The Bodge (1986) model was developed and tested from an impoundment study in a laboratory wave basin. Assuming a linear relationship between breaker height and water depth on a plane beach and ignoring wave setup, Bodge's (1986) model was simplified as

$$Q_i = kh_i^{1/2}V_i\left(\frac{dh}{dx}\right)_i^{3/2} \tag{17}$$

where Q = rate of LST; subscript i = local values; and k = dimensional coefficient. The energy dissipation, dH_b/dx, is simplified to local bed slope based on the $H_b = \gamma h$ assumption. The distribution longshore-current velocity was calculated based on the Longuet-Higgins (1970) model. By introducing a nondimensional parameter P to represent the relative importance of the lateral mixing

$$P = \frac{\pi Mm}{\gamma C_f} \tag{18}$$

Longuet-Higgins (1970) derived an analytical solution of longshore current distribution in the surf zone

$$V = B_1X^{P_1} + AX \tag{19}$$

where M = coefficient representing the strength of lateral mixing; $V = v/V_0$, V_0 is given by (13); v = local longshore current velocity; $X = x/x_b$; x_b = distance from the breaker line to the shore line; and B_1, A, and p_1 are functions of P. The mixing parameter, P, was adjusted to create a least-square fit with the measured data. It is apparent from (17) that the distribution pattern is strongly controlled by local beach slope.

The modeling results are summarized in Table 6. The distribution pattern of the LST rate is reproduced reasonably well for beaches with fairly uniform slope [Figs. 8(a) and 8(b)]. However, the accuracy decreases as the beach morphology becomes more complicated. Large errors are seen in the vicinity of plunge steps near the breaker line [Fig. 8(c)], which are common along low-energy, reflective coasts. The model is not capable of predicting the large LST rate measured in the swash zone [Fig. 8(d)]. Presumably, this is caused by the less accurate longshore-current calculation and, in part, by the fact that

TABLE 6. Summary of Measured and Calculated Cross-Shore Distribution of LST Rate from Energy-Dissipation (*E-E*) and Shear-Stress (*S-S*) Approaches

Location (number of data points) (1)	P[a] (2)	k[b] ($\times 10^5$) E-E (3)	k[b] ($\times 10^5$) S-S (4)	Standard Deviation $Q_{calculated}/Q_{measured}$ E-E (5)	Standard Deviation $Q_{calculated}/Q_{measured}$ S-S (6)
North Mantazas, Fla. (3)	0.95	17.55	0.081	0.10	0.54
Myrtle Beach, S.C. (5)	0.95	3.17	0.506	0.41	1.08
Emerald Isle, N.C. (4)	0.00	2.72	0.664	0.72	1.07
Jekyll Island, Ga. (3)	0.85	47.70	0.085	0.32	0.64
St. George Island, Fla. (3)	0.95	1.29	0.018	0.32	0.78
St. Joseph Island, Fla. (4)	0.85	5.09	0.017	0.32	0.92

[a]Mixing parameter that creates best fit with measured rate.
[b]Dimensional proportional coefficient, with units of kg/m$^{3.5}$, determined from field data.

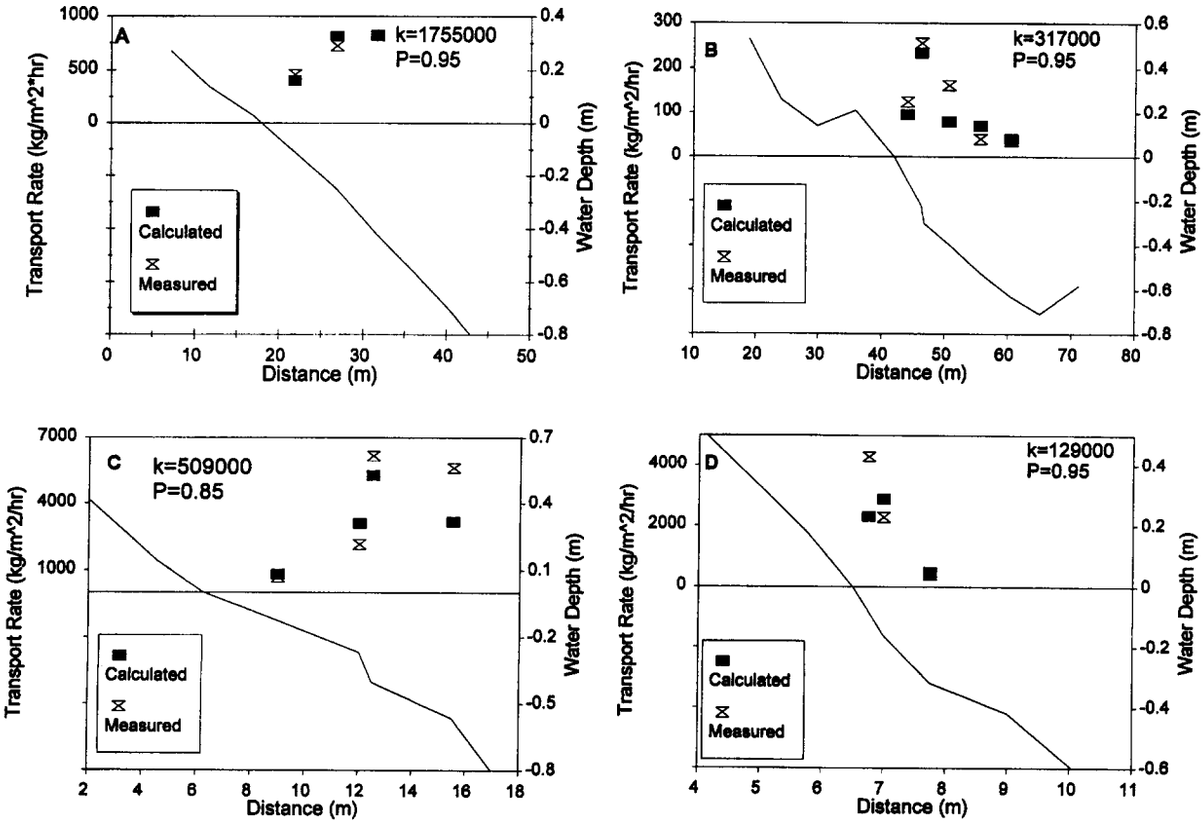

FIG. 8. Measured and Calculated Cross-Shore Distribution of LST Rate: (a) North Matanzas Beach, Fla.; (b) Myrtle Beach, S.C.; (c) St. Joseph Island, Fla.; (d) St. George Island, Fla.

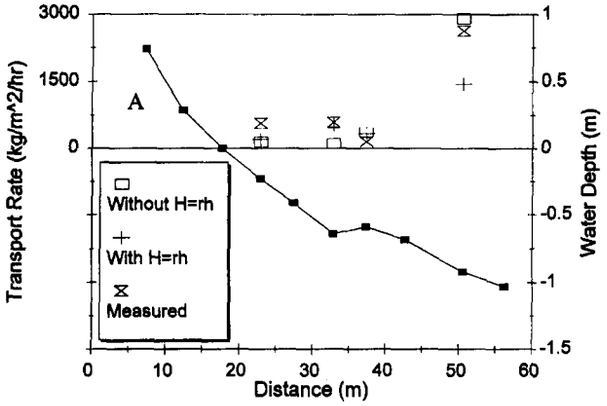

FIG. 9. Measured Cross-Shore Distribution of LST Rate and Prediction from Energy-Dissipation Approach (Bodge 1986). Mixing Parameter, $P = 0.00$, Proportional Constant $k = 272{,}000$ (with $H_b = \gamma h$) and 224,000 (without $H_b = \gamma h$), Respectively

the wave setup has been neglected. Notice the large error in the swash in Fig. 8.

The measurement at Emerald Isle, N.C. (Fig. 1, site 1), was conducted under higher wave-energy conditions as compared to the other measurements in this study (Table 1). The suspended-sediment concentration was found to be much higher at the breaker line, due to plunge breaking, than at other surf locations. The poor match between the calculated and measured distribution pattern was caused by the simplification of $H_b = \gamma h$, which significantly underestimated the influence of the large rate of energy dissipation at the breaker line. The transport at the breaker line is reproduced considerably closer to the measured value without the $H_b = \gamma h$ simplification (Fig. 9). The underprediction near the shoreline was probably caused by neglecting wave setup.

In summary, the Bodge (1986) model using an energy-dissipation approach predicted the LST distribution pattern reasonably well under low-wave energy conditions along a nonbarred coast. A large value of the mixing parameter, P, of around 0.9 seems to be more suitable for the low-energy settings. Under higher wave energy and plunging breakers in a wide surf zone, the simplification of $H = \gamma h$ underestimated the transport at the breaker line. Inclusion of the wave setup term may be important for assessing the swash-zone contribution. The dimensional parameter k was determined from the field data and varied from place to place.

Watanabe (1993) Model—Shear Stress Approach

A bottom shear-stress distribution in combination with the distribution of longshore-current velocity has been used to predict the local LST rate (Watanabe 1993). It is assumed that LST in the surf zone can be determined from the product of excess shear stress and local longshore-current velocity

$$Q_i = K_7 \rho(\Psi_i - \Psi_c) V_i \left(1 + \left(\frac{dH_b}{dx}\right)_i\right)^{k_5} \tag{20}$$

where K_7 and k_5 = dimensionless constants. The critical shear stress, Ψ_c, was much smaller than the actual Ψ, and was ignored. The wave friction factor, C_f, was canceled during the calculation of shear stress and longshore current velocity.

The results are summarized in Table 6. It has been shown in the previous sections that large transport rates often occur in places with coarser sediment in the same surf zone. The fact that the grain size, d, is in the denominator in (20) (through the calculation of the Shields parameter) indicates a negative relationship. This suggests that using the grain size of bottom sediment that may be the "relict" of sediment transport processes may be misleading.

One important factor that seems to have significant influence on LST distribution is the breaker type. Bodge (1986) and Bodge and Dean (1987) found from laboratory experiments that the distribution pattern was different under spilling and collapsing breakers. They found that more sediment tends to be transported in the swash zone under collapsing breakers. Similar situations were observed in the present field study. It is not possible to incorporate the descriptive breaker types into a quantitative analysis at present. The writer believes that part of the uncertainties in the modeling of both sediment flux in the water column and cross-shore distribution pattern were caused by the lack of distinction among different breaker types.

CONCLUSIONS

Distributions of sediment flux in the water column and across the surf zone are not uniform. Longshore sediment flux decreases logarithmically upward in the water column throughout the surf zone. The rate of upward decrease is largest in the trough and smallest in the swash.

The shape of the longshore sediment-flux profile in the water column can be described by a power function. Empirical modeling of the magnitude of the longshore flux from time-averaged energy flux, energy dissipation, and bottom shear-stress approaches is not satisfactory. The calculated profiles have similar shapes when compared with the measured profiles, but they have large variations in magnitude.

Six types of cross-shore distribution patterns of longshore sediment transport were recognized. A uniform distribution pattern was measured only under specific hydrodynamic and morphodynamic conditions. The distribution patterns are controlled by nearshore morphology, breaker-type, energy-dissipation pattern, and sediment properties. For low-energy coasts, the swash (nonbarred coast) and inner surf zone (barred coast) contain significant contributions to longshore sediment transport rate.

The cross-shore distribution pattern of longshore sediment transport for a plane beach was reproduced well using the energy-dissipation and shear-stress approaches developed mainly from laboratory studies. The relatively large errors found at the plunge step were caused by the less-accurate description of energy dissipation due to the abrupt slope change. Large errors in the swash zone were caused by the uncertainties in longshore current velocity prediction and neglecting wave setup. For a relatively narrow surf zone, the energy dissipation can be approximated by the local bed slope under low wave-energy condition.

ACKNOWLEDGMENTS

This study was funded by the Florida Department of Environmental Protection, Pinellas County, Fla., and the University of South Florida (USF). The writer would like to thank the graduate students in the Coastal Research Laboratory at USF for their assistance in the field work. The encouragement of Drs. Richard A. Davis Jr. and Nicholas C. Kraus is greatly appreciated. The support and review of an earlier version of the manuscript by Dr. Gregory Stone at Louisiana State University is also appreciated. The writer also thanks the reviewers and editor for a critical and helpful review of this paper.

APPENDIX. REFERENCES

Bailard, J. A. (1981). "An energetics total load sediment transport model for a plane sloping beach: local transport." *J. Geophys. Res.*, 86, 2035–2043.

Barkaszi, S. F., and Dally, W. R. (1993). "Fine-scale measurement of sediment suspension by breaking waves at Supertank." *Proc., 23rd Int. Conf. on Coast. Engrg.*, ASCE Press, New York, 1910–1923.

Bascom, W. N. (1951). "The relationship between sand size and beach-face slope." *Trans. AGU*, 32(6), 866–874.

Bodge, K. R. (1986). "Short term impoundment of longshore sediment transport," PhD thesis, Univ. of Florida, Gainesville, Fla.

Bodge, K. R. (1989). "A literature review of the distribution of longshore sediment transport across the surf zone." *J. Coast. Res.*, 5(2), 307–328.
Bodge, K. R., and Dean, R. G. (1987). "Short-term impoundment of longshore transport." *Proc., Coast. Sediment '87*, ASCE Press, New York, 468–483.
Bodge, K. R., and Kraus, N. C. (1991). "Critical examination of longshore transport rate amplitude." *Proc., Coast. Sediment '91*, ASCE Press, New York, 139–155.
Bosman, J. J., Van der Velden, E. T. J. M., and Hulsbergen, C. H. (1987). "Sediment concentration measurements by transverse suction." *Coast. Engrg.*, 11, 353–370.
Clifton, H. E. (1976). "Wave formed sedimentary structures." *Beach and nearshore sedimentation*, R. A. Davis Jr. and R. L. Ethington, eds., *SEPM Special Publication No. 24*, 126–149.
Dally, W. R., Dean, R. G., and Dalrymple, R. A. (1985). "Wave height variation across beaches of arbitrary profile." *J. Geophys. Res.*, 90, 11,917–11,927.
Dean, R. G. (1989). "Measuring longshore sediment transport with traps." *Nearshore sediment transport*, R. J. Seymour, ed., Plenum Publishing Corp., New York, 313–337.
Deigaard, R., Fredsoe, J., and Hedegaard, I. B. (1986). "Mathematical model for littoral drift." *J. Wtrwy., Port, Coast., and Oc. Engrg.*, ASCE, 112(3), 351–369.
Duane, D. B., and James, W. R. (1980). "Littoral transport in the surf zone elucidated by an Eulerian sediment tracer experiment." *J. Sedimentary Petrology*, 50, 929–942.
Ebersole, B. A., and Hughes, S. A. (1987). "DUCK85 photopole experiment." *Miscellaneous Paper CERC-87-18*, U.S. Army Engineer Waterways Experiment Station, CERC, Vicksburg, Miss.
Jonsson, I. G. (1966). "Wave boundary layers and friction factors." *Proc., 10th Int. Conf. on Coast. Engrg.*, ASCE Press, New York, 127–148.
Kamphuis, J. W. (1991a). "Alongshore sediment transport rate." *J. Wtrwy., Port, Coast., and Oc. Engrg.*, ASCE, 117(6), 624–641.
Kamphuis, J. W. (1991b). "Alongshore sediment transport rate distribution." *Proc., Coast. Sediments '91*, ASCE Press, New York, 170–183.
Kamphuis, J. W., Davies, M. H., Nairn, R. B., and Sayao, O. J. (1986). "Calculation of littoral sand transport rate." *Coast. Engrg.*, 10, 1–21.
Kana, T. W. (1979). "Suspended sediment in breaking waves." *Tech. Rep. No. 18-CRD*, Coast. Res. Div., Univ. of South Carolina, Columbia, S.C.
Komar, P. D. (1990). "Littoral sediment transport." *Handbook of coastal and ocean engineering*, J. B. Herbich, ed., Gulf Publishing Co., Book Div., Houston, Tex., 2, 681–715.
Komar, P. D., and Inman, D. L. (1970). "Longshore sand transport on beaches." *J. Geophys. Res.*, 75(30), 5514–5527.
Kraus, N. C. (1987). "Application of portable traps for obtaining point measurement of sediment transport rates in the surf zone." *J. Coast. Res.*, 2(2), 139–152.
Kraus, N. C., and Dean, J. L. (1987). "Longshore sediment transport rate distributions measured by trap." *Proc., Coast. Sediments '91*, ASCE Press, New York, 818–896.
Kraus, N. C., Gingerich, K. J., and Rosati, J. D. (1989a). "Toward an improved empirical formula for longshore sand transport." *Proc., 21st Int. Conf. on Coast. Engrg.*, ASCE Press, New York, 1183–1196.
Kraus, N. C., Gingerich, K. J., and Rosati, J. D. (1989b). "Duck85 surf zone sand transport experiment." *Tech. Rep. CERC-89-5*, U.S. Army Engineer Waterways Experiment Station, CERC, Vicksburg, Miss.
Kraus, N. C., Isobe, M., Igarashi, H., Sasaki, T. O., and Horikawa, K. (1983). "Field experiments on longshore transport in the surf zone." *Proc., 18th Int. Conf. on Coast. Engrg.*, ASCE Press, New York, 969–988.
Longuet-Higgins, M. S. (1970). "Longshore currents generated by obliquely incident waves, 1 and 2." *J. Geophys. Res.*, 75, 6778–6810.
Madsen, O. S., and Grant, W. D. (1976). "Sediment transport in the coastal environment." *Rep. No. 209*, Ralph M. Parsons Lab., Massachusetts Inst. of Technology, Cambridge, Mass.
Nielsen, P. (1984a). "On the motion of suspended sand particles." *J. Geophys. Res.*, 89, 616–626.
Nielsen, P. (1984b). "Field measurements of time-average suspended sediment concentration under waves." *Coast. Engrg.*, 7, 233–251.
Nielsen, P. (1986). "Suspended sediment concentrations under waves." *Coast. Engrg.*, 10, 23–31.
Rosati, J. D., and Kraus, N. C. (1988). "Hydraulic calibration of the streamer trap." *J. Hydr. Engrg.*, 114(12), 1527–1532.
Rosati, J. D., and Kraus, N. C. (1989). "Development of a portable sand trap for use in the nearshore." *Tech. Rep. CERC-89-11*, U.S. Army Engineer Waterways Experiment Station, CERC, Vicksburg, Miss.
Rosati, J. D., Gingerich, K. J., and Kraus, N. C. (1990). "Superduck surf zone sand transport experiment." *Tech. Rep. CERC-90-10*, U.S. Army Engineer Waterways Experiment Station, CERC, Vicksburg, Miss.
Rosati, J. D., Gingerich, K. J., and Kraus, N. C. (1991). "East pass and Ludington sand transport data collect project: data report." *Tech. Rep. CERC-91-3*, U.S. Army Engineer Waterways Experiment Station, CERC, Vicksburg, Miss.
Shore Protection Manual. (1984). U.S. Army Engineer Waterways Experiment Station, Coastal Engrg. Res. Ctr., U.S. Government Printing Office, Washington, D.C.
Sternberg, R. W., Shi, N. C., and Downing, J. P. (1989). "Continuous measurements of suspended sediment." *Nearshore sediment transport*, R. J. Seymour, ed., Plenum Publishing Corp., New York, 231–257.
Sunamura, T., and Kraus, N. C. (1985). "Prediction of average mixing depth of sediment in the surf zone." *Marine Geology*, Amsterdam, The Netherlands, 62, 1–12.
Thornton, E. B. (1973). "Distribution of sediment transport across the surf zone." *Proc., 13th Int. Conf. on Coast. Engrg.*, ASCE Press, New York, 1049–1068.
Van Rijn, L. C. (1984). "Sediment pickup functions." *J. Hydr. Engrg.*, ASCE, 110(10), 1494–1502.
Wang, P. (1995). "Surf zone sediment transport on low energy coasts: field measurement and prediction," PhD thesis, Dept. of Geol., Univ. of South Florida, Tampa, Fla.
Wang, P., and Davis, R. A. (1994). "Field measurement of longshore sediment transport rate in the surf zone: preliminary results." *Proc., 1994 Nat. Conf. on Beach Preservation Technol.*, Florida Shore and Beach Preservation Association, Tallahassee, Fla., 413–428.
Wang, P., Kraus, N. C., and Davis, R. A. Jr. (1998). "Total longshore sediment transport rate in the surf zone-field measurement and empirical predictions." *J. Coast. Res.*, 14, 269–282.
Watanabe, A. (1993). "Total rate and distribution of longshore sand transport." *Proc., 23rd Int. Conf. on Coast. Engrg.*, ASCE Press, New York, 2528–2539.
Zampol, J. A., and Inman, D. L. (1989). "Discrete measurement of suspended sediment." *Nearshore sediment transport*, R. J. Seymour, ed., Plenum Publishing Corp., New York, 257–285.